

Quantitative Human and Robot Motion Comparison for Enabling Assistive Device Evaluation*

Dana Kulić¹, Muhammad Choudry¹, Gentiane Venture², Kanako Miura³ and Eiichi Yoshida³

Abstract—A promising new application area for humanoid robots is in the area of assistive device testing. Humanoid robots can facilitate the experimental evaluation of assistive devices by providing repeatable, measurable, human-like motion while removing the difficulties and potential safety hazards associated with human trials. To ensure that the humanoid robot is providing a valid test platform, the robot must move in a similar way as a human while wearing the assistive device. This challenge is made difficult due to the inherent variability in human motion. In this paper, we propose an approach for a quantitative comparison between human and robot motion that identifies both the difference magnitude and the difference location, and explicitly handles both spatial and temporal variability of human motion. The proposed approach is demonstrated on data from robot gait and sagittal plane lifting.

I. INTRODUCTION

Recent research in robotics has expanded the use of robots beyond traditional industrial environments, into service and human home settings. Humanoid robots are well suited to these expanded applications, particularly for performing tasks currently performed by humans, due to their human like shape and motion capability [1]. Recently, several researchers [2], [3] have proposed the use of humanoid robots for evaluating assistive devices such as back braces and supports. Humanoid robots may be well suited to this application, as they can be used to reduce the need for expensive and potentially dangerous human trials, accelerate the design process and provide more extensive feedback.

In recent years, a wide variety of assistive devices have been proposed for assisting humans in their everyday life, both by academic researchers and industry. Potential applications include assisting the elderly or the disabled [4], [5], [6], preventing or reducing workplace injuries [7]. Two particular examples that are amenable to humanoid robot testing include walk support devices [4], [5], [2] and load-lifting assistive devices [8], of particular interest for reducing lower-back injuries, which are of significant concern in many occupations, such as transportation, agriculture and caregiving [9], [10].

*This work was supported by the Natural Sciences and Engineering Research Council of Canada and the Tokyo University of Agriculture and Technology Techno-Innovation Park.

¹D. Kulić and M. Choudry are with the Electrical and Computer Engineering Department, University of Waterloo, Canada [dana.kulic, muchoudr@uwaterloo.ca](mailto:dana.kulic,muchoudr@uwaterloo.ca)

²G. Venture is with the Department of Mechanical Systems Engineering, Tokyo University of Agriculture and Technology, Tokyo, Japan venture@tuat.ac.jp

³K. Miura and E. Yoshida are with the CNRS-AIST JRL (Joint Robotics Laboratory), UMI3218/CRT, AIST, Tsukuba, Japan e.yoshida@aist.go.jp

Miura et al. [3] propose an approach for using the HRP-4C robot to evaluate a torso-brace type assistive device which aims to reduce the torso torque during lifting. In the paper, human motion data of a participant lifting an object is first collected. The human motion data is converted to joint angles using inverse kinematics. The obtained joint angle trajectory is modified to ensure postural stability using the dynamics filter with preview control of Zero Moment Point (ZMP), fixing the ZMP in a single point relative to the ankle throughout the motion. The generated motion is compared to the human motion in terms of the angle of the torso and the relative angle between the torso and the upper leg to verify reproduction accuracy. An analytical model of the assistive device is also developed. The generated motion is performed on the humanoid robot, both wearing and not wearing the assistive device. The results show that torque at the torso is reduced when wearing the assistive device, however, the analytical model does not predict the experimental results accurately. This paper highlights the benefit of using robot experimental data rather than analytical models alone. However, the proposed approach does not take into account the possibility that the human may change their movement strategy as a result of wearing the device. The comparison metric between the human and the robot motion is also manually selected (only two joint angles).

In order to enable this new application, the robot must be able to perform the movement in the same manner as the human, and therefore a quantitative comparison between robot and human motion is required. This comparison is made difficult due to the temporal and spatial variability of human motion. Even when performing the same movement under the same conditions, human motion will exhibit variability, both in terms of the path traversed to complete the motion and in terms of the exact timing along the path. In addition, it may not be sufficient to compare the motion only in the affected joint (i.e., the torso for back bracing), as the addition of the brace may cause the human to adapt their movement in joints away from the intervention site [11].

In this paper, we propose an approach for motion comparison between the human and robot motion that is capable of capturing both the spatial and temporal variability of human motion, and can perform whole body comparison of the movements. The proposed approach is based on a stochastic dynamic modeling of human and robot movement, and a distance measure evaluated at each degree of freedom of the movement. The proposed approach is validated on two datasets: a gait movement and lifting movement datasets. Results show that the proposed approach is able to identify

differences in the motion profile between the robot and the human which may impact assistive device evaluation.

II. MOTION COMPARISON APPROACH

A. Motion Modeling

To compare the robot movement with the human movement, we adapt the approach originally proposed by Choudry et al. [11], [12] for comparing human movements. Here, each movement is modeled by a Hidden Markov Model (HMM) [13], which models the temporal evolution of the movement as a stochastic process. The HMM modeling approach is illustrated in Figure 1. Each HMM λ is composed of three parameters:

$$\lambda = (\pi, A, B)$$

where π is the initial state probability vector, A is the state transition matrix, and B is the probability distribution function. For modeling individual movements, left-to-right HMMs are used so that $\pi_1 = 1$. Each element a_{ij} of the state transition matrix describes the probability that the model will transition to state j at time t given that the model was previously in state i at time $t-1$. The probability distribution function for each state i is defined as a multivariate Gaussian:

$$b_i = \mathcal{N}(\mu_i, \Sigma_i)$$

where μ_i and Σ_i are the mean and covariance, respectively.

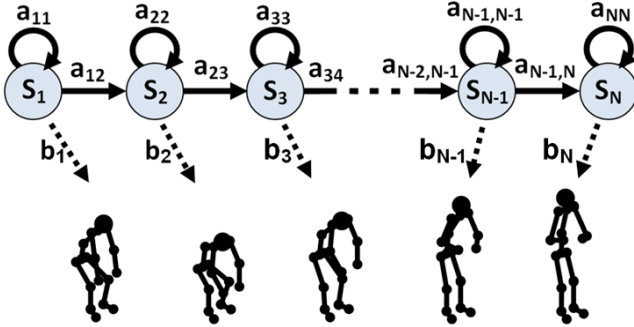


Fig. 1: HMM Modeling of Movement Data

To model each movement, a set of training motion sequences are required. The parameters for the model λ are initialized, assuming all the states are of equal duration, and initializing the probability distribution function parameters by computing the means and variances of equally sized windows distributed over the length of the sequences, as proposed in [14]. The Baum-Welch algorithm [13] is then used to train the model from the data.

B. Motion Comparison

Given two movement models, λ_1 and λ_2 , the distance between them can be computed based on the Kullback-Leibler (KL) divergence:

$$D(\lambda_1, \lambda_2) = \frac{1}{T} [\log P(O^1 | \lambda_1) - \log P(O^1 | \lambda_2)] \quad (1)$$

where O^1 is an observation sequence generated from λ_1 , $P(O|\lambda)$ is the probability that an observation sequence O was generated by model λ , and T is the length of the observation sequence. $P(O|\lambda)$ is computed via the forward algorithm [13]. The KL distance is not symmetric, a symmetric distance can be obtained by computing the average of the distance obtained with respect to each model:

$$D_s(\lambda_1, \lambda_2) = \frac{D(\lambda_1, \lambda_2) + D(\lambda_2, \lambda_1)}{2} \quad (2)$$

The KL distance performs a computation of the distance between two movements incorporating information both about the distance between prototypical movements from each set of exemplars, and the variability of the movement exemplars. For example, for a movement with very small variability, an observation sequence that deviates from the prototypical movement will result in a low probability that the movement is generated by the model, $P(O|\lambda)$, resulting in a larger distance. On the other hand, a movement which has large variability during execution will generate large $P(O|\lambda)$ for a larger variety of movements.

The KL distance described above provides a single, scalar measure of distance between two movements. To identify which body segment or joint is contributing to the overall difference between two movements, excluded DoF analysis [11] or included DoF analysis [12] can be applied. We use the included DoF analysis in this paper. In this approach, two HMM motion models are selected, and the KL distance is computed for each DoF separately. This analysis can be carried out each for a single DoF, or for groups of DoFs. The DoF or group of DoFs that results in the largest distance is the DoF that is the most different between the two motion models.

C. Comparison Between Robot and Human Movements

In this paper, we wish to compare movements performed by the human demonstrator and similar movements performed by the humanoid robot, in order to quantitatively evaluate the effectiveness of the motion re-targeting approach, and determine whether the robot's motion effectively models the human movement such that it can be used to evaluate assistive devices. The approach described above is general and can be applied to any time series data. For the comparison between human motion and robot motion, different signal sources can be considered: Cartesian data of the locations of the joints or limbs, joint angle data of a kinematic model, or force torque data. To enable force torque data comparison, forces/torques of the human at each joint must be estimated from motion capture, EMG and contact force data [15], based on a dynamic model of the body [16] and an appropriate muscle model [17].

Due to the difficulty in accurately estimating joint torques from kinematic measurements and/or EMG data, in this paper we focus on the first approach. Specifically, we compare the human and the robot motion data by comparing trajectories of the Cartesian locations of the joint centres of the robot and the human. This comparison enables a direct

comparison between the measured data of human motion and robot motion. In this case, the distance metric (Eq. 2) describes the distance between the human and the robot time series data in terms of Cartesian values. The distance metric is a unitless value that incorporates both spatial and temporal differences between two sets of time series. For a single DoF comparison, if there are no temporal differences, a distance value of 1 indicates that the time series, represented as a set of key poses along the trajectory, are separated from each other by one standard deviation in Cartesian space. The standard deviation is computed from the variability in the human and robot movement observed from multiple demonstrations of the same task.

III. EXPERIMENTS

The proposed approach is tested on two datasets, a gait dataset [18] and a lifting dataset [3]. For each dataset, pre-processing is applied to extract the individual movement segments and generate comparable time series Cartesian data for comparison. The approach described in Section II is then applied to perform a quantitative analysis of the differences between the robot and human movement.

A. Datasets

1) *Gait Dataset*: In this dataset, one female human demonstrator performed two walking movements at different speeds, one at 0.83 and one at 1.15 sec/step. Each walking movement consisted of five strides. The movement of the human demonstrator was recorded using the Vicon motion capture system, using the marker locations shown in Figure 2. The movement of the human demonstrator was re-targetted to the HRP-4C humanoid robot [19] using the approach proposed in [18], as illustrated in Figure 3. Joint angles of the robot while performing the movement were collected.

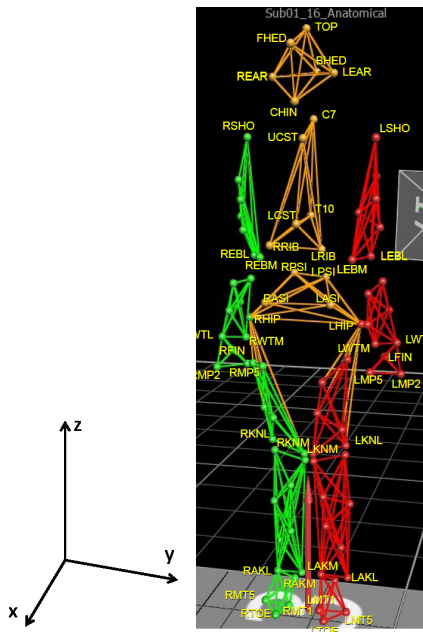


Fig. 2: Marker Locations and Frame Assignment



Fig. 3: Illustration of the gait dataset [18].

2) *Lifting Dataset*: In this dataset, a male human demonstrator performs a sagittal lifting movement, lifting a weight from the ground to waist height. The weight is distributed evenly between the two hands, with 3kg carried at each hand. The movement of the human demonstrator was recorded using the Vicon motion capture system, using the marker locations shown in Figure 2. Three movement repetitions were recorded. The movement is re-targetted on the HRP-4C humanoid robot using the approach proposed in [3]. The robot performs the movement while wearing the "Smart Suite Lite" assistive device [8], designed to reduce lower back loading, and wearing 1kg weight wrist straps at each wrist. Joint angles of the robot while performing the movement were collected. The data collection and re-targetting process is illustrated in Figure 4.

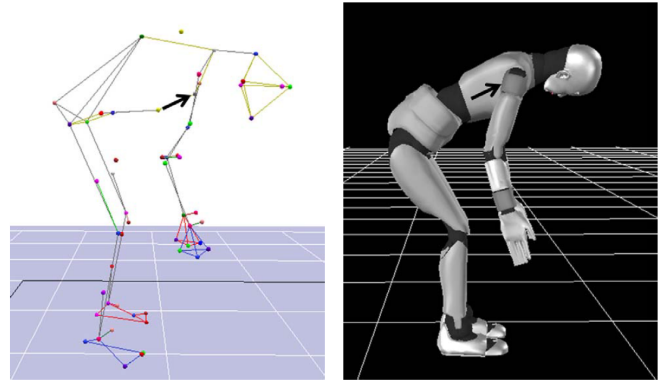


Fig. 4: Illustration of the Lifting dataset [3]

B. Data Preprocessing

1) *Segmentation*: For the gait dataset, the data consisted of multiple strides in sequence. This data was first segmented to extract individual strides. The segmentation was carried out automatically by considering the trajectory of the right toe. The Cartesian data of the right toe was first low pass filtered and then differentiated to compute the velocity. The velocity signal was scanned to find negative to positive velocity crossings (i.e., time instances where the velocity changed from negative to positive). Each stride was extracted as the data segment between two adjacent negative to positive zero velocity crossings. The same segmentation procedure was applied to both the human and the robot data. The automated segmentation was manually validated to remove spurious

incomplete segments due to noise; only complete, correctly segmented strides were used for subsequent analysis.

2) *Forward Kinematics and Data Alignment*: For the Cartesian data comparison, the Cartesian locations of the joint centres of the following joints were considered: torso, left and right knee, hip, ankle, toe, shoulder, elbow and wrist. Two types of analysis were performed: 3 DoF analysis, where the Cartesian data (x,y,z) of each joint is considered as a group, and 1 DoF analysis, where each Cartesian dimension (i.e., the x , y , and z direction) is considered separately. For the human gait dataset, for one of the strides (normal speed walking), the human demonstrator was at the edge of the capture space, and some of the markers were not visible. This stride was excluded from subsequent analysis. For the robot data, joint locations were computed using the forward kinematics of the robot. For multi DoF joints (e.g., hip, shoulder), the average of the axis centres of the 1DoF components was computed.

For the human data, the measured Cartesian positions were rotated and translated to align the data into the robot-centered frame and the locations of the joint centres were computed by averaging the locations of the lateral and medial markers for the knee, ankle, elbow and wrist. For the gait dataset, the data was additionally scaled in the z -direction based on the ratio of the robot to human right shoulder height with respect to the hip centre in the first frame. This scaling was applied to account for the difference in height between the human demonstrator and the robot.

For the lift dataset, data was additionally normalized for each joint to remove the average starting offset, such that each trajectory represented the joint movement from the average starting position.

IV. RESULTS

A. Gait Dataset

For the gait dataset four motion types were compared. Two of the motion types were generated by the robot (referred to as Robot1 and Robot2) and the other two were generated by a human (referred to as Human1 and Human2). The data for each of these 4 motions were used to train HMM models and the KL-distance between each of the models were computed (shown in Table I).

TABLE I: Distance Matrix for the Gait Dataset

	Human1	Human2	Robot1	Robot2
Human1	0	0.31	0.24	0.24
Human2	0.31	0	0.35	0.35
Robot1	0.24	0.35	0	0.0037
Robot2	0.24	0.35	0.0037	0

Visual inspection of the data indicates that the Robot1 and Robot2 movements are very similar to each other with low variation. This is confirmed by Table I, where the Robot1-to-Robot2 distance is the smallest in the table. This also meets expectations since it is expected that the robot movement will contain much lower variance than human movement.

Comparing the two human datasets, Human1 and Human2 have similar gait features but the Human2 stride is about 2 times longer in duration than the Human1 stride. In principle if the stride is exactly the same but slower, the HMM models and distance computation should be able to account for this difference and identify the two motions as being very similar, which is confirmed by our analysis. In order to look at the differences in more detail an Included-DoF analysis was performed, shown in Figures 5 and 6. In the Included-DoF analysis, we re-computed the distances between the movements considering either the 3DoF position of each joint separately (multi-DoF analysis), or considering each (x,y,z) direction separately (1 DoF analysis).

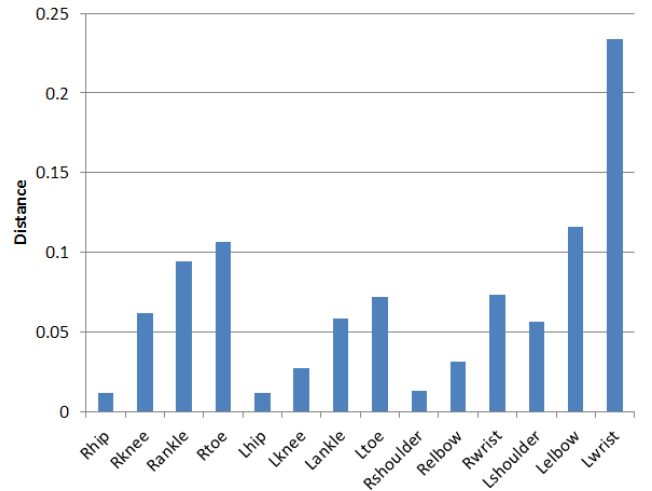


Fig. 5: Included-Multi-DoF Analysis for Human1 vs Human2 for the Gait Data

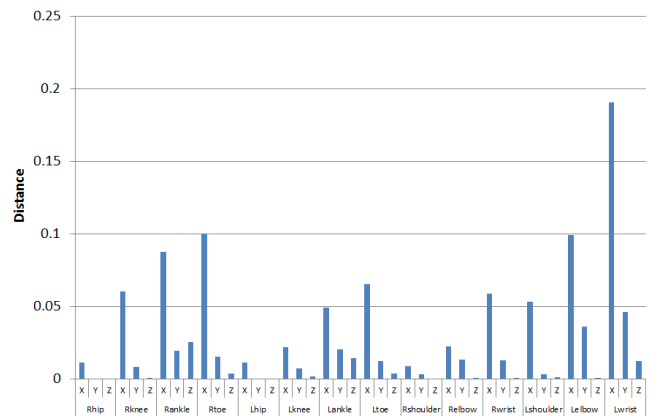


Fig. 6: Included-Single-DoF Analysis for Human1 vs Human2 for the Gait Data

The included-DoF analysis between Human1 and Human2 indicates that distances are progressively increasing going from the hip to the toe joints as well as when going from the shoulder to the wrist. This trend appears to be symmetric on the left/right side joints and appears to be due to differences in the x -axis direction. The differences are due to differences in the gait appearance as a result of differences in gait speed (for the slower Human2 motion the stride is slightly larger

and the amplitude of the swinging of the arms is lower). One exception is the wrist where the human2 motion appears to have an asymmetry between the positioning of the left and right wrist, as can be seen from Figures 7 and 8. One hypothesis could be that the slower walking is not as natural to the human demonstrator, which may prevent natural and symmetric arm swinging.

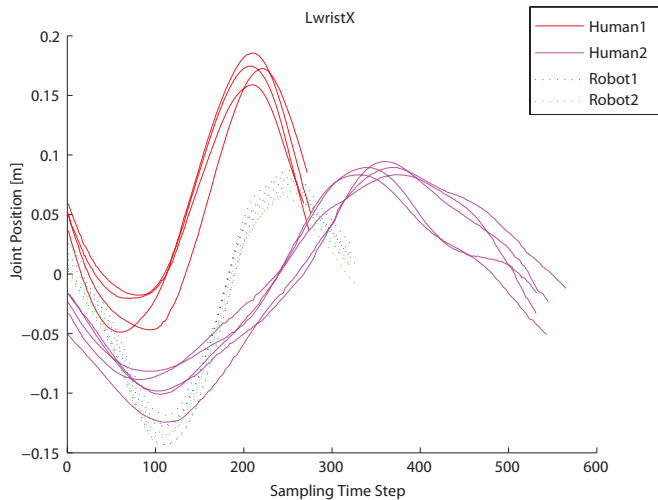


Fig. 7: Left Wrist Trajectories for the Gait Data

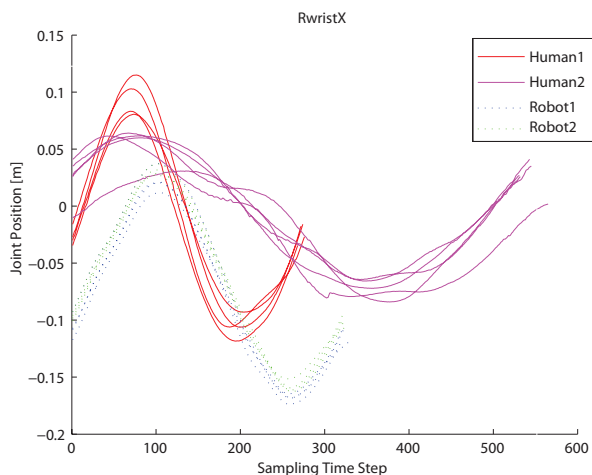


Fig. 8: Right Wrist Trajectories for the Gait Data

We next compared Human1 motions against the Robot motions (the choice of robot motion does not matter as they were nearly identical). The graphs indicate large differences in the wrist which can be traced to differences in the z-axis. This difference is due to different heights at which the wrist is held between the human and the robot during the gait stride (mostly an offset difference). This difference is due to the re-targetting strategy [18], where the wrist is held further away from the body than the human movement to avoid self-collisions.

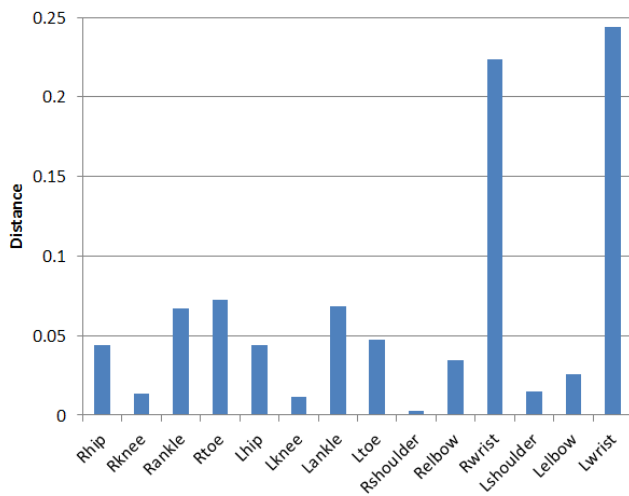


Fig. 9: Included-Multiple-DoF Analysis for Human1 vs Robot1 for the Gait Data

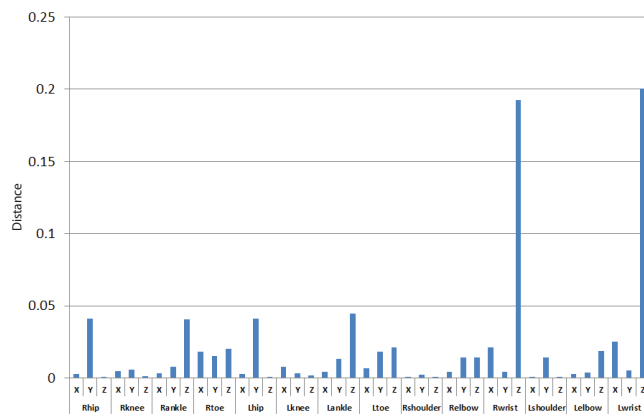


Fig. 10: Included-Single-DoF Analysis for Human1 vs Robot1 for the Gait Data

Comparing the human and the robot data for the lower body, differences are observed in the toe, ankle and hip, with much less difference in the knee. This is as expected, as the goal of the walking re-targetting strategy is to emulate knee extended (human-like) walking [18]. The difference in the y-axis at the hip is due to an offset in marker locations - the robot's hip is measured at the joint center while the human hip is measured at the surface of the body. At the toe, the magnitude of the movement is different between the robot and the human, with the robot having a slightly larger forward stride (x-axis). In the y-axis, there are also differences between the time the robot and the human reach peak displacement in the toe trajectory, while the overall trajectory shape is the same.

B. Lifting Dataset

For the lift data set we are comparing human motions against robot motions. From visual inspection the robot motions have fairly low variation between each other whereas the human motions have slightly higher temporal variation between each other. From the Included-DoF analysis (Figure 11 and 12) we find the largest magnitude differences are in

the upper body. This is to be expected as the re-targetting approach [3] focused more closely on tracking the lower body (torso and thigh incline angles). For the most part the differences in the upper body are due to differences in magnitude of the trajectory, as can be seen in Fig. 13 for the left wrist.

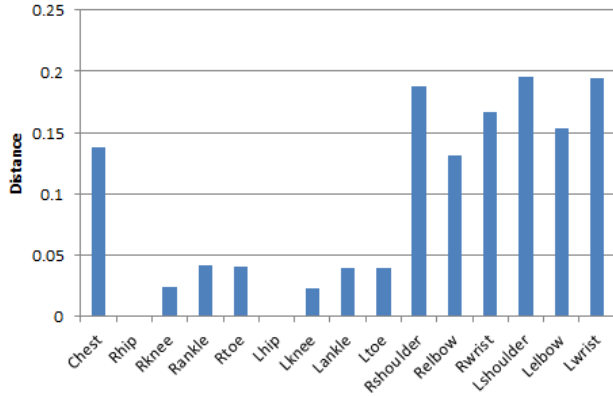


Fig. 11: Included-Multiple-DoF Analysis for Human vs Robot for the Lift Data

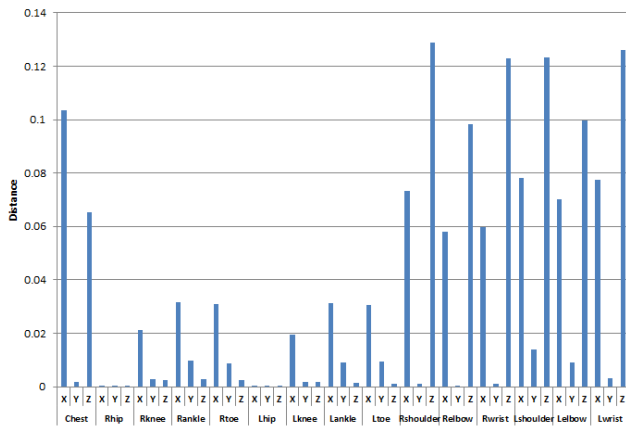


Fig. 12: Included-Single-DoF Analysis for Human vs Robot for the Lift Data

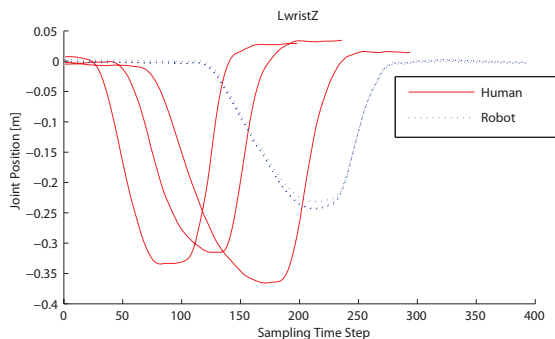


Fig. 13: Wrist Trajectories for the Lift Data

There are also smaller but non-negligible differences in the lower body movements. Significantly for the analysis of assistive device testing, there are differences in the magnitude of chest movement, with the robot's movement being lower in magnitude in both the X and Z directions. Finally, smaller

differences are detected in the toe, ankle and knee trajectories in the forward (X) direction (Fig. 14), with the human and robot motions having similar range but a different temporal profile. These differences might be significant when utilizing the robot as an assistive device evaluator, as differences in the trajectory profile might result in different loading patterns.

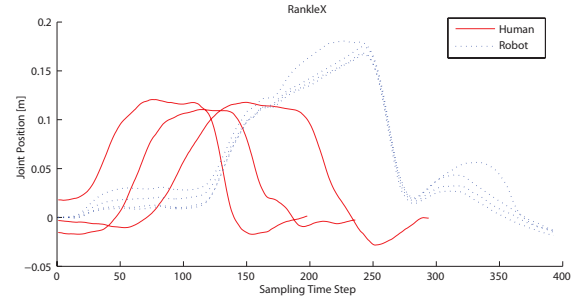


Fig. 14: Ankle Trajectories for the Lift Data

V. DISCUSSION

The analysis above indicates that differences may persist between human and robot motion, even when robot motion is designed to emulate human movement. Particularly when only a subset of the joints are used for emulating human movement, it is likely that unintended differences may occur in the remaining joints. These differences may be important during assistive device evaluation, as they may lead to movement and loading patterns differences between the human and the robot.

The proposed approach provides a scalar quantification of the difference between human and robot motion. This quantification may be useful for designing strategies that minimize the difference between human and robot motion. It should be noted that the difference between human and robot motion can be due to differences between the human and humanoid anatomy, kinematic and dynamic constraints, and other factors in addition to the re-targetting strategy, in which case even the optimum re-targetting strategy may not reduce the distance to zero. As the anatomy and kinematic structure of HRP-4C is close to the human one (within 10% of average Japanese young women [19]), the influence of anatomic and kinematic factors is reduced, making it easier to identify differences due to re-targetting and control strategies.

An important aspect of assistive device evaluation is the human adaptation to the assistive device. To ensure that the humanoid robot accurately evaluates the assistive device, the humanoid should correctly imitate both movement without the use of the device, initial use of the device, and expert (adapted) use of the device. An important role of the evaluation is the static supportive effect for load-supporting devices. Since it is difficult to quantitatively evaluate the torque applied to the lower back for humans with EMG or other physiological measures, evaluation through a humanoid can provide an important guideline. The development of adaptation models is an important area of future work. The proposed approach can be used to evaluate the validity of the adaptation model.

In the current paper, we analyze differences between human and robot movements in Cartesian space. When using Cartesian data, scaling to account for differences in height between users and the robot must be applied. In this work, we applied a simple approach, based simply on a single scale factor in the vertical (z) axis based on the difference between the human model and the robot. A more complete approach that incorporates the avoidance of self-collisions, is the work of Nakaoka and Komura [20]. While the analysis in Cartesian space developed here reveals differences between movements, further research is needed to understand how differences between movements influence differences in loading patterns.

VI. CONCLUSIONS AND FUTURE WORK

Humanoid robots are a promising technology for evaluating assistive devices, as they can repeatably wear and test the devices without introducing the difficulties and safety considerations of human trials. However, to produce reliable evaluation results, the humanoid motion must be demonstrated to be comparable to human motion. This paper proposed an approach for comparison between human and robot motion, considering simultaneously the spatial and temporal characteristics of the full body motion and taking human variability into account. The analysis on replicative movements carried out to date demonstrates the importance of considering the full body motion during the analysis, as methods which consider imitation based only on a few ad-hoc selected joints may introduce unintended differences between the human motion and the robot motion, which may impact the validity of the evaluation of the assistive device.

In future work, we hope to examine the validity of the proposed approach for joint angle and torque data, and to develop re-targetting strategies which minimize the difference between human and robot movement patterns. The evaluation of on-going adaptation will also be considered.

ACKNOWLEDGMENT

The authors wish to thank Dr. Masaaki Mochimaru and Mr. Kei Aoki of the Digital Human Research Center, AIST, for providing us with the captured human motions.

REFERENCES

[1] C. C. Kemp, P. Fitzpatrick, H. Hirukawa, K. Yokoi, K. Harada, and Y. Matsumoto, "Humanoids," in *Springer Handbook of Robotics*, B. Siciliano and O. Khatib, Eds. Springer Berlin Heidelberg, 2008, pp. 1307–1333.

[2] A. M. Omer, H. Kondo, H. Lim, and A. Takahashi, "Development of walking support system based on dynamic simulation," in *Proc. 2008 IEEE Int. Conf. on Robotics and Biomimetics*, 2008, pp. 137–142.

[3] K. Miura, E. Yoshida, Y. Kobayashi, Y. Endo, F. Kanehiro, K. Homma, I. Kajitani, Y. Matsumoto, and T. Tanaka, "Humanoid robot as an evaluator of assistive devices," in *IEEE International Conference on Robotics and Automation*, 2013, pp. 671–677.

[4] Toyota Corporation, "Walk assist robot," http://www.toyota-global.com/innovation/partner_robot/family_2.html#h203, 2013, [Online; accessed Aug 2013].

[5] H. Kawamoto, S. Lee, S. Kanbe, and Y. Sankai, "Power assist method for hal-3 using emg-based feedback controller," in *IEEE International Conference on Systems, Man and Cybernetics*, 2003, pp. 1648 – 1653.

[6] Y. Kume and H. Kawakami, "Control technology of RoboticBed for supporting independent life,," Panasonic, Tech. Rep., 2010.

[7] H. Kobayashi and H. Nozaki, "Development of muscle suit for supporting manual worker," in *IEEE/RSJ Int. Conf. on Intelligent Robots and Systems*, 2007, p. 17691774.

[8] Y. Imamura, T. Tanaka, Y. Suzuki, K. Takizawa, and M. Yamanaka, "Motion-based-design of elastic material for passive assistive device using musculoskeletal model," *Journal of Robotics and Mechatronics*, vol. 23, no. 6, pp. 978–990, 2011.

[9] E. K. Wai, D. M. Roffey, P. Bishop, B. K. Kwon, and S. Dagenais, "Causal assessment of occupational lifting and low back pain: results of a systematic review," *The Spine Journal*, vol. 10, p. 554566, 2010.

[10] S. M. Hsiang, G. E. Brogmus, and T. K. Courtney, "Low back pain (lbp) and lifting technique - a review," *Int. J. of Industrial Ergonomics*, vol. 19, p. 5974, 1997.

[11] M. Choudry, M. Pillar, T. Beach, D. Kulić, and J. P. Callaghan, "Detecting changes in human motion using stochastic distance measures," in *IEEE Engineering in Medicine and Biology Conference*, 2011, pp. 3475 – 3478.

[12] M. U. Choudry, T. A. C. Beach, J. P. Callaghan, and D. Kulić, "A stochastic framework for movement strategy identification and analysis," *IEEE Transactions on Human-Machine Systems*, vol. 43, no. 3, pp. 314 – 327, 2013.

[13] L. R. Rabiner, "A tutorial on hidden Markov models and selected applications in speech recognition," *Proceedings of the IEEE*, vol. 77, no. 2, pp. 257–286, 1989.

[14] D. Kulić, G. Venture, and Y. Nakamura, "Detecting changes in motion characteristics during sports training," in *IEEE Engineering in Medicine and Biology Conference*, 2009, pp. 4011 – 4014.

[15] Y. Nakamura and K. Yamane, "Dynamics computation of structure-varying kinematic chains and its application to human figures," *IEEE Trans. on Robotics and Automation*, vol. 16, no. 2, p. 124134, 2000.

[16] G. Venture, K. Ayusawa, and Y. Nakamura, "Motion capture based identification of the human body inertial parameters," in *IEEE Engineering in Medicine and Biology Conference*, 2008, pp. 4575–4578.

[17] F. Zajac, "Muscle and tendon: Properties, models, scaling, and application to biomechanics and motor control," *Crit. Rev. Biomed. Eng.*, vol. 7, p. 359411, 1989.

[18] K. Miura, M. Morisawa, F. Kanehiro, S. Kajita, K. Kaneko, and K. Yokoi, "Human-like walking with toe supporting for humanoids," in *Proc. 2011 IEEE/RSJ Int. Conf. on Intelligent Robots and Systems*, 2011, pp. 4428–4435.

[19] K. Kaneko, F. Kanehiro, M. Morisawa, K. Miura, S. Nakaoka, and K. Yokoi, "Cybernetic human HRP-4C," in *Proc. 2009 IEEE-RAS Int. Conf. on Humanoid Robots*, 2009, pp. 7–14.

[20] S. Nakaoka and T. Komura, "Interaction mesh based motion adaptation for biped humanoid robots," in *IEEE-RAS Int. Conf. Humanoid Robots*, 2012, pp. 625 – 631.